STUDY OF CLAY-CEMENT SLURRIES WITH MECHANICAL AND ELECTROMAGNETIC WAVES

By M. A. Fam[1] and J. C. Santamarina,[2] Associate Member, ASCE

ABSTRACT: This paper describes the results of a test program in which the setting and hardening of cement, bentonite-cement slurries, and attapulgite-cement slurries are monitored in the laboratory with mechanical-shear and electromagnetic waves. Specimens are prepared by prehydrating the clay before adding cement. The presence of clays in soil-cement slurries delays hydration and its manifestation. The complex permittivity emerges as a sensitive indicator of ongoing reactions. Permittivity reflects changes in the mobility of water, liberation and entrapment of ions, changes in specific surface, and variations in double-layer phenomena. The increase in shear-wave velocity reflects the rise in effective stress due to consolidation, the decrease in double-layer repulsion, and the higher rigidity of the mixture as a result of cementation. Early stages of hydration denoted by changes in permittivity do not contribute to the formation of a rigid, cemented network. Overall, it is shown that the simultaneous measurement of permittivity and shear-wave velocity provides complementary microlevel information on the fundamental dependency between chemical reactions, physical changes, and rigidity in cementitious materials. The application of these results to field situations will lead to the development of nonintrusive, nondestructive monitoring techniques.

INTRODUCTION

Almost 20 centuries ago, the Greeks and Romans used lime to protect their roads. Early this century, cement, bitumen, and chemicals were mixed with or injected into geomaterials to enhance their properties (e.g., to increase strength or to lower permeability). Due to current needs for waste storage sites and the containment of contaminants, further developments in soil stabilization are required to meet these new demands.

In the case of cutoff walls, slurries serve two functions: to stabilize trench walls and to act as cutoff barriers. The evaluation of clay-cement slurry walls comprises the assessment of proper construction (e.g., continuity and homogeneity), the control of hydration and hardening (including shrinkage, settlement, and stress relaxation), and the evaluation of long-term effects due to freeze-thaw cycles or to the continued exposure to harsh chemicals. Current tests are either based on invasive techniques or require sampling. In both cases, only local information is provided.

Waves have been successfully applied to monitor concrete and cement hydration and to assess structural integrity [e.g., Laine et al. (1980); Berthaud (1991)]. However, no systematic study has been made to evaluate the use of waves in monitoring the evolution of soil-cement slurries or in monitoring field applications of stablized clayey soils, such as walls and liners around landfills. The ability to detect improper construction, inadequate performance, and changes in the long-term behavior of barriers using these techniques would be most beneficial to engineering practice. The purpose of this paper is to study clay-cement slurries during setting and hardening, through the use of nondestructive mechanical-shear and electromagnetic waves. Results can lead to the development of noninvasive techniques that can only assess clay-cement materials, but also can provide global-spatial information.

[1]Grad. Student, Dept. of Civ. Engrg., Univ. of Waterloo, Ont., Canada N2L 3G1.

[2]Assoc. Prof., Dept. of Civ. Engrg., Georgia Inst. of Technol., Atlanta, GA 30332-0355; formerly Assoc. Prof., Dept. of Civ. Engrg., Univ. of Waterloo, Ont., Canada N2L 3G1.

Note. Discussion open until October 1, 1996. To extend the closing date one month, a written request must be filed with the ASCE Manager of Journals. The manuscript for this paper was submitted for review and possible publication on April 7, 1995. This paper is part of the ***Journal of Geotechnical Engineering***, Vol. 122, No. 5, May, 1996. ©ASCE, ISSN 0733-9410/96/0005-0365–0373/$4.00 + $.50 per page. Paper No. 10492.

FUNDAMENTAL CONCEPTS AND PRIOR STUDIES

This section reviews fundamental concepts in cement hydration, soil-cement interaction, and prior studies with mechanical and electromagnetic waves.

Cement, Clay, and Clay-Cement Slurries

Dry cement is produced by partial melting of silicates, aluminates, and carbonates into a "clinker," which is later pulverized into 1–50 μm angular particles. The chemical composition is: tricalcium silicate C_3S, dicalcium silicate C_2S, tricalcium aluminate C_3A, and calcium ferroaluminate C_4AF, where C = CaO; S = SiO_2; A = Al_2O_3; and F = Fe_2O_3.

Basic physical and chemical processes in cement hydration can be explained by changes at the molecular level, which include changes in structure, reactions with water, and products of chemical reactions. Hydration involves two mechanisms (Mehta 1986; Taylor 1990). The first one occurs during the early stages, and encompasses the solution of individual components and the formation of hydrates. The secondary mechanism is "solid state hydration," whereby reactions take place at the surface, without solution; this mechanism prevails at later stages. The formation of specific chemical compounds can be grouped into three consecutive phases of hydration. The physical and chemical characteristics of each phase are described in Table 1.

Clays differ in properties such as particle size and shape, mineralogical constitution, lattice expansion, specific surface (surface area of 1 g of dry soil), and cation exchange capacity. A comparative listing of these properties for bentonite and attapulgite is summarized in Table 2 (the tabulated properties correspond to the soils used in this study). Differences in crystalline structure and particle shape between bentonite and attapulgite have significant effects on their behavior.

Clay-cement slurries can be prepared by prehydrating the clay, or by dry-mixing clay and cement first. Bentonite-cement slurries with optimal conditions for impermability, flexibility, and resistance, incorporate 5–7% bentonite by weight with respect to the total weight of the slurry, and 1:2 bentonite-to-cement ratio (Leonards et al. 1985).

The evolution of low-water content clay-cement mixtures during hydration was studied by Mitchell and El Jack (1965). During the early stages of curing, calcium silicate hydrate C-S-H begins to form and the clay is transformed into a calcium-clay through ion exchange with calcium ions produced by cement hydration. The high pH accompanying cement hydration

TABLE 1. Different Phases in Cement Hydration [Summarized from Taylor (1990); Mehta (1986)]

Time (h) (1)	Chemical characteristics (2)
Less than 3	Reaction between C_3A and calcium sulfate ⇒ gel layer around particles. Ettringite nucleates at particle edges (near the aluminate phase). Delayed nucleation of C-S-H and/or CH ⇒ induction period. Increase in $[Ca^{2+}]$, $[K^+]$, $[Na^+]$, $[SO_4^{2-}]$, $[Al_2O_3]$, and $[OH^-]$.
3–24	Reaction of C_3S ⇒ rapid formation of CH and C-S-H. Strong heating takes place. C-S-H ⇒ porous shell around cement grains on the ettringite. Renewed reaction of the aluminate phase ⇒ more ettringite is formed. Renewed growth of ettringite ⇒ decrease in $[Ca^{2+}]$ and $[SO_4^{2-}]$.
Greater than 24	Continuous decrease in shell permeability ⇒ deposition of C-S-H. Ettringite ⇒ monosulfate. Diffusion controls the hydration rate ⇒ decrease in reactions rate. Only K^+, Na^+, and OH^- in the pore fluid can be detected at this stage. The specific surface area increases from 0.3 to 0.4 m^2/g for dry cement to 100–200 m^2/g for well-hydrated pastes.

TABLE 2. Main Characteristics and Differences of Bentonite and Attapulgite

Soil type (1)	Bentonite (2)	Attapulgite (3)
Source	Saskatchewan	Floridin Co., Florida
Trade name	Avonseal or Geoseal	Florigel H-Y
Wet color	Light green	Cream
Particle shape	Flake-laminar	Needle
Crystal structure	Three-layer sheet	Double chain
Specific gravity, G_s	2.55	2.55
Specific surface, m^2/g	400	330
LL (deion) (%)	250	346
LL (1 M NaCl) (%)	100	256
Plastic limit (%)	50	100
pH value	9.0 (5% solids)	9.8 (5% solids)
CEC (meq/100 g)[a]	80–85	20–30
Electrophoresis (5% solids)	Strong attraction to the positive electrode	No attraction to the positive electrode
(*a*) Pore fluid analysis		
Main cation	Sodium	Magnesium
Mixing water content	600%	670%
Method of extraction	Centrifuge (10,000 rpm)	Centrifuge (2,000 rpm)
Na (ppm)[b]	427.10	6.30
K (ppm)	7.40	1.83
Mg (ppm)	17.50	35.80
Ca (ppm)	19.55	3.25
Total (ppm)	471.55	47.18

[a]CEC cation exchange capacity (provided by distributor).
[b]These values were obtained by ion chromatography on extracted fluid.

favors the solubility of SiO_2 and Al_2O_3, which interact with the CaO from the hydrated cement, and additional cementing materials precipitate. This process results in a rapid consumption of line (CaO) compared to the hydration of cement without clay (Kezdi 1979). As the curing time increases, discrete soil and cement particles loose identity. This is also the case in high-water-content bentonite-cement slurries (Plee et al. 1990): a discontinuous microstructure with cavities forms gradually, and after few hours, the presence of the clay phase cannot be distinguished due to the appearance of the C-S-H phase.

The main pore fluid properties that control clay behavior are: concentration, valence, pH, and permittivity (Fang et al. 1992; Santamarina and Fam 1995). Cement hydration is accompanied by an increase in pH and Ca^{++} ion concentration (Suzuki et al. 1981). Hence, the interaction of clays with hydrating cements is significantly affected by these factors (Plee et al. 1990). The increase in pH during cement hydration is an additional advantage to clay-cement slurry walls in landfill applications, since a higher pH facilitates the precipitation of heavy metals (Yong and Phadungchewit 1993).

The increased concentration of Ca^{++} in pores cause shrinkage of the double layer leading to flocculation and an increase in permeability. However, pores may be blocked, for example by pozzolanic cement substances (Broderick and Daniel 1990). The hydraulic conductivity of bentonite-cement slurries decrease with time [from $1.2 \cdot 10^{-8}$ to $3 \cdot 10^{-9}$ m/s in 30 days—flexible wall permeameter by Chapuis et al. (1984)]. Permeability measurements in different clay-cement slurries with water and methylene chloride permeants suggest that attapulgite-cement has the highest resistance to dense nonaqueous phase liquid (DNAPL) attack compared to other typical slurries (Sai and Anderson 1992). Hence, it appears that the use of attapulgite instead of bentonite in slurry walls would result in a more chemically resistant wall, at least for some chemicals. Millet et al. (1992) reported that attapulgite is stable in the presence of salts; however, it is not able to produce the filter case adjacent to unstable soils, like sands. Slag cement is an alternative mix component; it produces a lower calcium concentration in the pore fluid than cement, thus it is expected to reduce the flocculation of bentonite (Trivedi et al. 1992).

Electromagnetic Properties of Soil and Cement

Dielectric permittivity characterizes the response of a material to a traveling electromagnetic wave. Permittivity is a complex parameter, κ^*; the real component, κ', reflects the polarizability of the material due to the application of an electric field. It is related to the number of dipole moments per unit volume. The imaginery permittivity, κ'', characterizes Ohmic and polarization losses (Hasted 1973)

$$\kappa^* = \kappa' - i\kappa'' \tag{1}$$

There are several polarization mechanisms, including electronic and ionic resonance, orientational polarization, double-layer polarization, and spatial Maxwell-Wagner relaxation (Chelkowski 1980; Fam and Santamarina 1995). The permittivity at GHz frequencies reflects the volumetric amount of free water. On the other hand, the complex permittivity at lower frequencies gives information about the absorbed water, and about the displacement of charges and their entrapment at interfaces (Santamarina and Fam 1995). The resulting spatial polarization depends on the conductivity of the different components in the mixture; hence, it can reflect changes in the composition of the phases or in the mobility of ions. The polarization of the material κ' increases monotonically from high to low frequencies.

The complex permittivity of cement is very sensitive to the water-cement ratio. Changes in permittivity upon hydration have been investigated by several researchers, in different frequency ranges (Tamas 1982; McCarter and Curran 1984; Moukwa et al. 1991; Xie et al. 1993; and others). Two peaks in the conductivity versus time plot have been identified with measurements at kHz frequencies (Tamas 1982). The first peak starts early upon the addition of water and denotes the presence of Ca^{++}, OH^-, SO_3^{--}, and alkali ions that went into solution by hydrolysis. Similar observations were made by Moukwa et al. (1991) with measurements at 10 GHz. The

TABLE 3. Long-Term and Short-Term Testing Programs

Test number (1)	Test symbol (2)	Material[a] (3)	Mixing ratio (clay:cement) (4)	Water content (% by weight of clay)[b] (5)	Duration S/L[c] (6)
1	A-1-0.1-15	Attapulgite: cement	1:0.1	1,500	L
2[d]	A-1-1-31	Attapulgite: cement	1:1	3,100	S and L
3[d]	A-1-2-31	Attapulgite: cement	1:2	3,100	L
4	B-1-0.1-12	Bentonite: cement	1:0.1	1,200	S and L
5[d]	B-1-1-23	Bentonite: cement	1:1	2,300	S and L
6[d]	B-1-2-23	Bentonite: cement	1:2	2,300	L
7[d]	Impermix	Attapulgite: slag cement	—	454[e]	S and L
8[d]	Cement	Cement	—	40–43	S and L

Note: B = bentonite; A = attapulgite; and 1-1-12 = ratio of clay: cement:water.

[a]Mixing order: (clay + water) + cement.

[b]Selected to reflect similar fluidities—no specific control test was conducted.

[c]L = Long-term test in the curing cell, S = short-term test in the oedometer.

[d]Duplicates monitored at regular intervals.

[e]Percent by weight of the mix.

second peak occurs after 7 hours and corresponds to the transformation of ettringite to monosulfate. McCarter and Curran (1984) also observed a second peak in permittivity at 1 kHz, 8 hours after hydration (w/c = 0.40). However, at 10 GHz, a decrease in conductivity is observed apparently due to a general decrease in the mobility of water, which has become part of the hydration products (Moukwa et al. 1991). They also noted that conductivity and permittivity increase as the water-cement ratio increases. Higher conductivity levels are related to higher degrees of supersaturation of the lime solution together with higher hydroxyl concentrations.

The interaction of electromagnetic waves with clays depends on the clay type (shape, specific surface, and cation exchange capacity) and on pore fluid properties (dielectric permittivity, concentration, and fluid content). Further details on electromagnetic wave-clay interaction can be found in Mitchell and Arulanandan (1968) and Wensink (1993).

Early measurements by Smith and Arulanandan (1981) of low-water content kaolinite-cement mixtures at 1–100 MHz indicate an increase in permittivity and a corresponding decrease in conductivity with hydration time for a mixture with 0.24 cement/clay ratio. The writers are not aware of any comprehensive evaluation of clay-cement slurries with electromagnetic waves.

Low-Strain Dynamic Properties of Soil and Cement

The velocity and attenuation of mechanical waves in particulate materials are controlled by the state of stress and by factors such as particle geometry, void ratio, and packing. Several experimental studies have been conducted to analyze the effect of the state of stress on shear-wave velocity V_S (Schultheiss 1981; Viggiani and Atkinson 1995). It has been shown that V_S is controlled by the effective stresses in the directions of propagation and polarization (Roesler 1979). Santamarina and Fam (1995) showed that shear-wave propagation in fine-grained soils depends on the net interparticle force, which is affected by the change in pore fluid chemistry. Changes in the pore fluid affect both double-layer repulsion and van der Walls attraction and, therefore, influence shear-wave velocity. Low-strain shear stiffness, G, is related to the shear-wave velocity, V_S by

$$V_S = \sqrt{\frac{G}{\rho}} \tag{2}$$

where ρ = mass density of the material.

Mechanical waves have been used to nondestructively test the integrity of concrete structures, and to assess cement hydration. Matsufuji and Kawakami (1984) measured shear-wave velocity in cement paste and observed a sharp increase in the velocity-time plot upon the beginning of initial setting. Wilding and Double (1984) used compressional waves and made a similar observation: velocity showed a low time rate of increase for the first 2 to 3 hours, followed by a high rate. The transition time coincides with the beginning of the initial setting. The high rate of increase in velocity takes place as the paste loses plasticity and the internal network begins to form. The same behavior was observed during hydration of tricalcium silicate pastes (Lawrence et al. 1977). The use of P-waves to study cement hydration is not relevant during early stages of hydration since water is the stiffer component. Compressional waves can be used when the skeleton stiffness exceeds the stiffness of water. Once again, the writers are not aware of systematic studies of clay-cement slurries with mechanical waves.

EXPERIMENTAL WORK

This section describes the experimental methodology and devices used to study and monitor the setting and hardening of clay-cement slurries with electromagnetic and mechanical waves. Complementary tests were also performed, and are briefly described. Field conditions have been simulated regarding materials, mixing percentages, and procedure.

Tested Materials

Two types of clay were used: bentonite and attapulgite. Properties of the clays and extracted pore fluids are presented in Table 2. Case histories documented in the literature show a wide range of cement content (cement weight/soil weight), from 6% in the case of subgrade stabilization to 350% in some slurry walls, and a wide variation in moisture content (weight of water/weight of solids) for slurry-wall mixtures, ranging from 200% to more than 800% (Kezdi 1979; Jefferis 1981). In this study, the water content was selected to provide similar viscosities upon mixing (no specific control test was used). A commercially available mixture of attapulgite and slag cement was also tested (Impermix, produced by Liquid Earth Support, Inc., New York).

Testing Program and Devices

The battery of tests included exploratory sedimentation studies in test tubes, short-term tests in an oedometer (temperature, complex permittivity, and shear-wave velocity; duration three to 12 days), long-term tests in curing cells (complex permittivity; duration ≈ two years), hydration temperature, and pH in curing cells (duration 3 to 12 days). The tested mixtures are summarized in Table 3. The cell used in short-term tests was an oedometer modified to include all required transducers. Details of this cell and peripheral devices can be found in Fam and Santamarina (1995). The oedometric cell was placed within a styrofoam enclosure to minimize the effect of external thermal fluctuation. The vertical stress was kept at a constant nominal value of σ_v = 1.50 kPa. The du-

ration of these tests was restricted by the accelerated corrosion or the short circuiting of buried transducers.

Cylindrical plexiglas curing cells, 40 mm high and 50 mm in diameter, were used for long-term tests. Sixteen samples were prepared representing eight different mixtures, and were kept in the same humidifier to provide an identical curing environment. Careful sample preparation and measuring procedures were adopted to minimize noise in data. The continuous monitoring with embedded tranducers in the oedometric cell produced excellent, virtually noiseless results, which were used to corroborate the quality of curing-cell data.

The measurement of the dielectric permittivity in both short-term and long-term cells was conducted with a coaxial dielectric probe connected to a HP-8752A network analyzer. This system covers the frequency range from 0.02 GHz up to 1.30 GHz. The shear-wave velocity was determined with piezoelectric bender elements operating between 1 and 100 kHz (Santamarina and Fam, in press, 1996). Finally, temperature changes during hydration were monitored with thermocouples embedded in specimens.

RESULTS OF EXPLORATORY STUDY: MIXING ORDER

Preliminary exploratory tests to select the most suitable water content for each slurry showed the remarkable effect of mixing order. Further assessment of this phenomenon was based on sedimentation tests in cylindrical flasks. These tests were conducted at low solid-liquid concentrations, allowing maximum interplay of interparticle forces with minimum mechanical constraint. Hence, sedimentation results highlight the effect of long-range forces and the formation of different fabrics. Procedure and results follow (these tests were repeated on several occasions and under a variety of conditions leading to the same results).

Clay salt: The sedimentation of 1 g of oven-dry bentonite was examined under three different conditions. In test 1, bentonite was mixed with 40 mL of distilled water. In test 2, bentonite was mixed first with 40 mL of water and left to hydrate for one day; then calcium chloride $CaCl_2$ was added to form a 0.10 M solution. In test 3, bentonite was mixed with 40 mL of 0.10 M solution of $CaCl_2$. After one day, the three tubes were vigorously shaken and the sedimentation volumes were measured with time. The results presented in Fig. 1(a) emphasize the difference between the two mixing orders. The sedimentation volume in test 3 reached equilibrium very fast (within 20 min). On the other hand, equilibrium took place after four days in test 2, with a sedimentation volume five times greater than that of test 3. Similar sedimentation tests with varying ions and concentration confirmed these results (e.g., KCl), which are in agreement with Jefferis (1992). An identical set of sedimentation tests was performed with attapulgite, following the same procedures and material proportions [Fig. 1(b)].

Clay cement: Two low-concentration soil-cement slurries were tested. The first one was prepared by prehydrating the clay and then adding cement (wet-mixing). The second slurry was made by dry-mixing cement and clay and then adding water (dry-mixing). Each slurry contained 1 g of dry clay, 1 g of cement, and 200 mL of distilled water. Sedimentation test results for bentonite cement are shown in Fig. 2(a), and for the attapulgite-cement slurry in Fig. 2(b). The effects of mixing order are the same in both mixtures. Similar to what was observed with the sedimentation of clay salt, prehydrated clays have a slow sedimentation rate and produce higher sedimentation volumes. On the other hand, the presence of larger cement particles, which are positively charged, accelerates the rate of sedimentation, as compared to the clay salt in Fig. 1(a), yet not as fast as the sedimentation of cement alone, which occurs within 1 min.

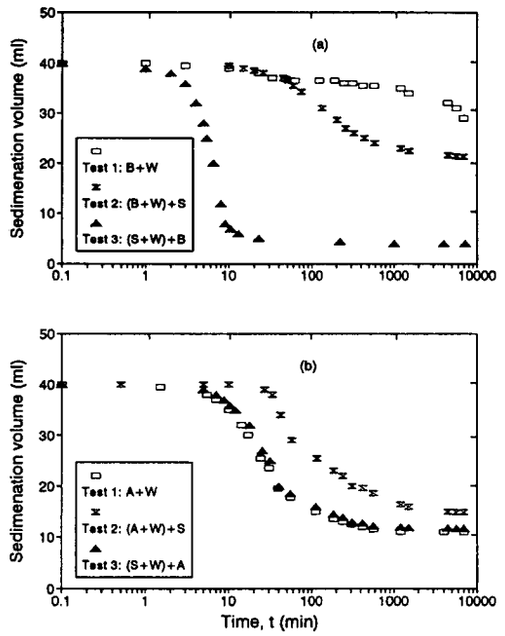

FIG. 1. Sedimentation Test and Mixing Order (No pH Change); Clay Slurries Prepared with Distilled Water and 0.15 M $CaCl_2$ Solution: (a) Bentonite in $CaCl_2$; (b) Attapulgite in $CaCl_2$

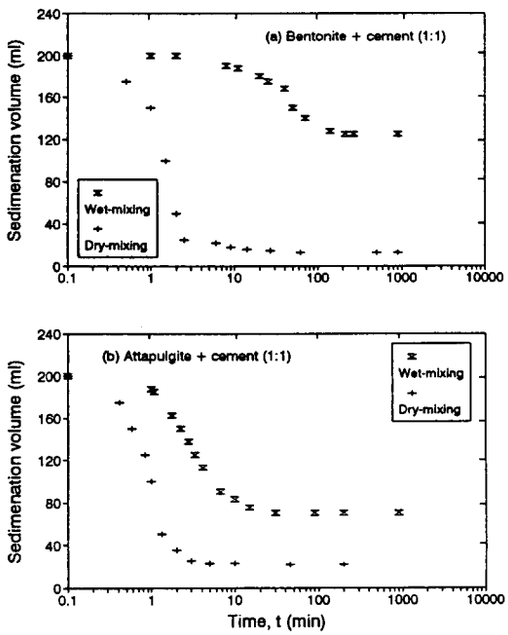

FIG. 2. Sedimentation Tests of Clay-Cement Slurries Prepared by Prehydrating Clay and Adding Cement (Wet-Mixing) and by Dry-Mixing Clay and Cement and Adding Water: (a) Bentonite; (b) Attapulgite (Cement Presence Increases pH; End Volumes Reflect Fabrics)

To further assess the implications of wet-mixing and dry-mixing, two specimens of bentonite cement B-1-1-23 were prepared with different mixing order (numbers indicate the relative weight of clay, cement, and water). After mixing, the electromagnetic loss, κ'', and pH were recorded with time. The evolution of the measured parameters is presented in Fig. 3(a). The wet-mixed slurry shows a rapid increase in both pH and κ'' compared to the dry-mixed slurry (the pH of cement is 12.4 immediately upon adding water). Data from a similiar study with attapulgite are shown in Fig. 3(b). In this case, there is no difference in conductivity or pH between the two mixing orders.

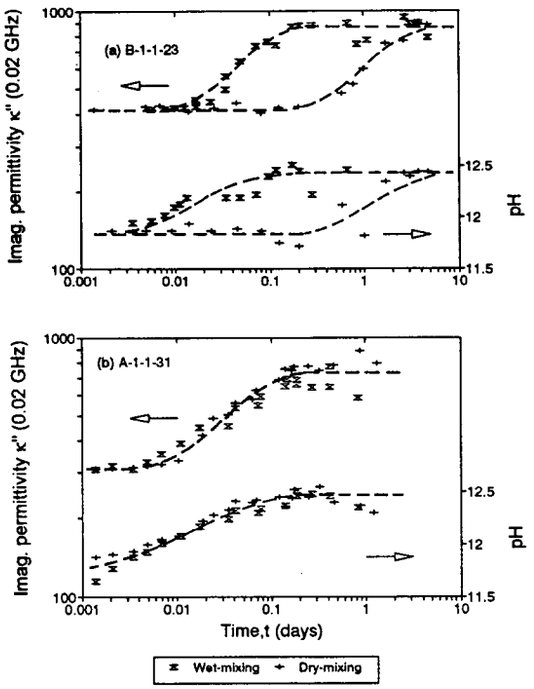

FIG. 3. Rate of Reactions and Mixing Order; Evolution of Imaginary Permittivity and pH for Wet-Mixing and Dry-Mixing: (a) Bentonite Cement; (b) Attapulgite Cement

TABLE 4. Final Properties of Slurries and Cement

Material (1)	Cement (2)	B-1-1-23 (3)	B-1-2-23 (4)	A-1-1-31 (5)	A-1-2-31 (6)	Impermix (7)
Water content (%)	—	780	470–570	1,168	714–820	320
Shear-wave velocity (m/s)[a]	2,100	125	130	70	115	1,500
Undrained shear strength (kPa)[b]	—	240	280–320	60	120–140	—
Permittivity at surface (0.02 GHz)[c]	3.8, 0.5	94, 66	93, 81	86, 180	112, 140	44, 32.9
Permittivity at center (0.02 GHz)[c]	—	110, 330	160, 650	172, 200	130, 650	103, 183
Permittivity at surface (1.30 GHz)[c]	3.6, 0.3	39, 4.7	31, 5.7	53, 6.5	37, 6.9	25, 3.1
Permittivity at center (1.30 GHz)[c]	—	65, 10	58, 16	55, 7.5	60, 15	60, 7.5

Note: All data presented in this table were measured 2 years after mixing. The differences between measurements on the surface and at the center of the split sample are due to probe penetration and moisture gradients.

[a]The uncertainty in V_s from curing cell samples is about 10%.

[b]Values obtained using vane shear test at the middle of the specimen.

[c]3.8, 0.5 = real and imaginary permittivity, respectively.

RESULTS OF SHORT- AND LONG-TERM TESTS

The following sections describe the change in measured parameters during hydration, for both short-term and long-term tests. Final measurements for mechanical and electromagnetic parameters are summarized in Table 4. To facilitate comparison, data are also presented for the portland cement used to prepare the slurries.

Cement (w/c = 0.40)

Temperature: The temperature inside the cement specimen showed two peaks: the first one occurred 10 min after mixing and the second one 8 hours later [see also McCarter and Curran (1984)].

Dielectric permittivity: The change in real and imaginary permittivity κ' and κ'' with time are summarized in Fig. 4 for three different frequencies. Values are normalized with respect to t_0-measurements. The change in permittivity shows two peaks within the first 2 hours and it is almost complete within one day from mixing. The first peak occurs after 4 min, which corresponds to the beginning of initial hydration. After this peak, a decrease in permittivity is observed reflecting the end of the first hydration stage. The significant differences in real κ' and imaginary κ'' permittivities between 0.02 and 1.30 GHz should not be overlooked. The fact that κ' at 0.02 GHz exceeds the value of the real permittivity for water $\kappa' = 78$ indicates spatial polarization within the mixture, which is affected by ionic mobility. The high values of the imaginary permittivity κ confirm high ionic content and mobility, and overshadows the polarization losses of free water ($\kappa'' =$ six for free water at 1.30 GHz). The real permittivity κ' at 0.02 GHz shows more pronounced peaks and then decays faster than κ' at 1.30 GHz; therefore, ionic changes are even more severe than changes in the polarizability of water.

Shear-wave velocity: Fig. 5(a) summarizes the evolution of shear-wave velocity, V_S, during the hydration of the cement paste. The increase in V_S is limited during the first 2 hours. Afterwards, V_S increases at a high rate for the following 12 hours.

Bentonite Cement

The prehydrated bentonite-cement slurry was placed in the oedometer under 1.50 kPa vertical stress. The vertical strain reached 3.5% and stabilized after 5 hours.

Temperature: All components were at room temperature before mixing, $T = 22°C$. Immediately after mixing a 3–4°C increase in temperature resulted from mechanical mixing and early cement hydration. A temperature peak was observed 90 min after hydration. Thereafter, the temperature inside the cell decreased monotonically to room temperature.

Dielectric permittivity: Fig. 6 shows the time variation of the complex permittivity at three frequencies 0.02, 0.10, and 1.30 GHz. At a high frequency (1.30 GHz), the real permittivity decreases monotonically. However, the real permittivity κ' at 0.02 GHz increases to very high polarizability values after 1 hour and does not decay for the first 20 days. End values remain high for all frequencies including 1.3 GHz,

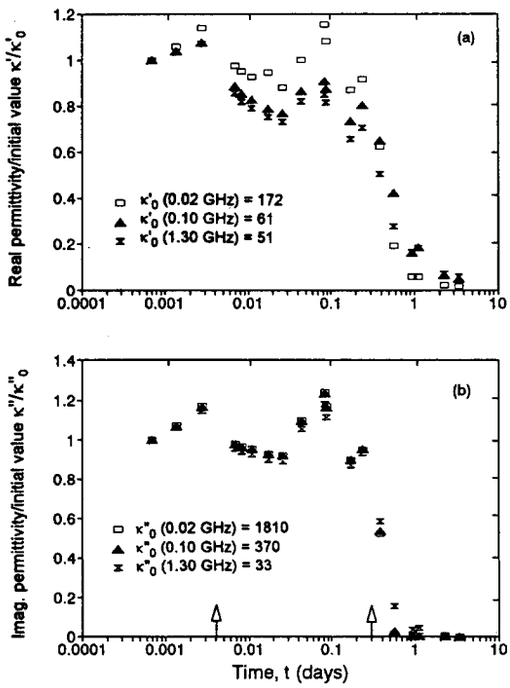

FIG. 4. Change in Complex Permittivity of Cement Paste (w/c = 0.40) with Hydration Time, at Three Frequencies: (a) Real; (b) Imaginary (Permittivity Values Are Normalized by Initial Values; Arrows Denote Time of Temperature Peaks)

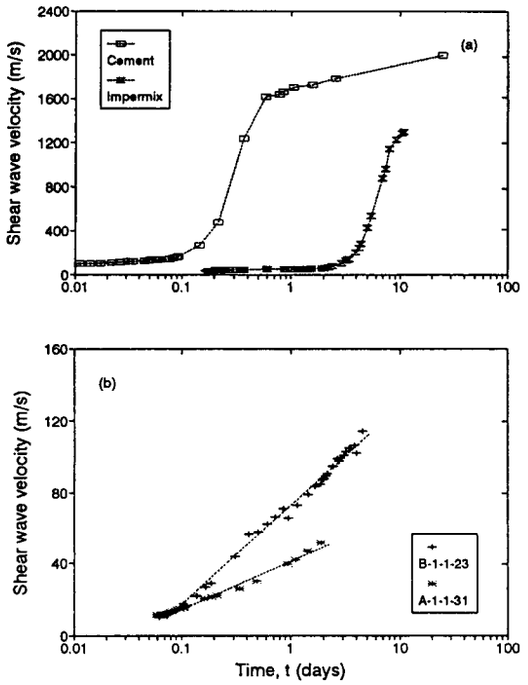

FIG. 5. Evolution of Shear-Wave Velocity with Hydration Time: (a) Cement (w/c = 0.40) and Impermix; (b) Bentonite Cement and Attapulgite Cement

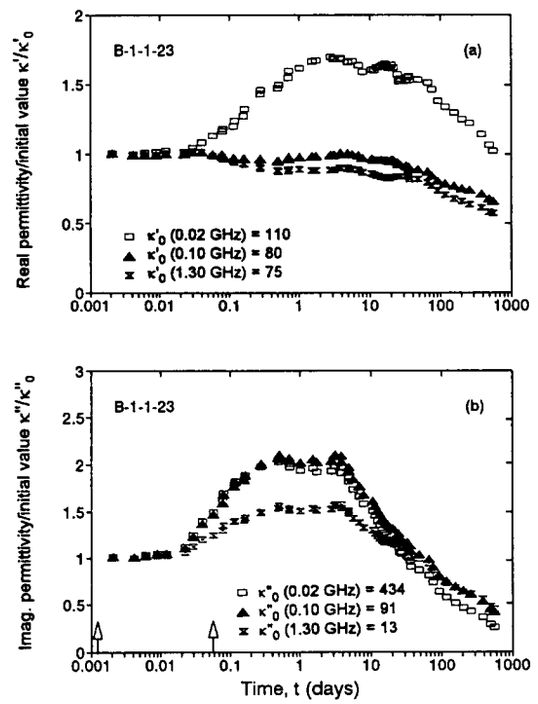

FIG. 6. Change in Complex Permittivity of Bentonite-Cement Slurry (B-1-1-23) with Hydration Time, at Three Frequencies: (a) Real; (b) Imaginary (Permittivity Values Are Normalized by Initial Values; Arrows Denote Time of Temperature Peaks)

highlighting the massive presence of free water. Times for temperature peaks are shown in Fig. 6(b).

The change in imaginary permittivity shows different stages [Fig. 6(b)]. First, there is a slow increase in κ'' with time that lasts approximately 30 min when early hydration begins to take place. Then, κ'' increases decisively from 5 to 12 hours, reflecting further reactions among components. We have observed that the higher the cement content, the longer the duration of this stage and the higher the values of κ'' at 0.02 GHz. Two minor peaks in κ'' occur after 12 hours and three days, and they are more prominent at lower frequencies. Finally κ'' decreases steeply at all frequencies after the three days.

Shear-wave velocity: Shear-wave velocity in clay-cement slurries was measured in the oedometric cell, and a long-term value was obtained from curing cells (shown in Table 4). The shear-wave velocity of bentonite slurry (no cement) consolidated to 1.5 kPa is less than 10 m/s. The addition of 10% cement increases V_S to 20 m/s. Data in Fig. 5(b) shows that 1:1 bentonite-cement slurry can reach $V_S \approx 120$ m/s, at the same consolidation pressure of 1.50 kPa (one-week velocities). Hence, cement produces changes in initial fabric (minor increase in t_0-velocity) and a rigid cemented matrix that increases the low-strain shear stiffness and V_S. Fig. 5(b) is plotted in semi-logarithmic scale, thus the increase in velocity with time occurs at a gradually decreasing rate.

Attapulgite Cement

Temperature: No clear temperature peaks could be observed during the hydration of the attapulgite-cement slurry; however, an initial increase in temperature was measured just after mixing.

Dielectric permittivity: Time changes in real and imaginary permittivity are shown in Fig. 7. General trends are similar to the case of bentonite cement (Fig. 6). The initiation of active hydration occurs at about the same time. The most salient difference is the slower rate of final decay in κ'' with respect to bentonite cement, indicating significant residual ionic mobility after two years.

Shear-wave velocity: The change in shear-wave velocity with hydration time for 1:1 attapulgite-cement slurry is shown in Fig. 5(b). The initial shear-wave velocity is similar to bentonite; however, velocity does not increase as much in the attapulgite-cement slurry as in the bentonite-cement slurry. In

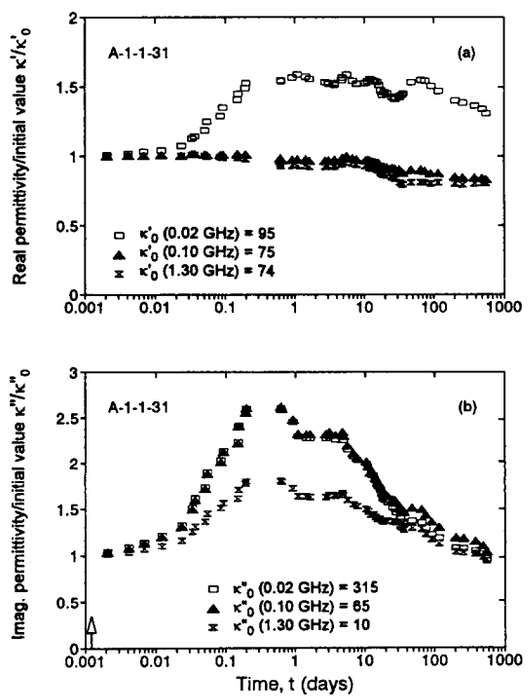

FIG. 7. Change in Complex Permittivity of Attapulgite-Cement Slurry (A-1-1-31) with Hydration Time, at Three Frequencies: (a) Real; (b) Imaginary (Permittivity Values Are Normalized by Initial Values; Arrow Denotes Time of Temperature Peak)

part, this may be due to the higher water content, which reduces both long-term rigidity and strength.

Impermix

This material was different from the earlier clay-cement mixtures starting with the earliest observations during mixing (smell, bleeding, and sedimentation into an extremely soft deposit at early stages).

Temperature: The change in temperature during the hydration of impermix was similar to that of the attapulgite-cement slurry.

Dielectric permittivity: Results are shown in Fig. 8. Initial permittivity values indicate the preponderant effect of water, i.e., $\kappa' = 78$ and $\kappa'' = 6$ for $f = 1.30$ GHz. Values for lower frequencies indicate some incipient double-layer effects or spatial polarization. Hydration and ion liberation is very gradual, reflecting a peak in ionic concentration/mobility after 10 days. The decay in κ' and κ'' takes place afterwards, and the mix becomes very hard (color changes to greenish). Under these conditions, surface measurements of κ^* become difficult. Final, midsample κ^* values are significantly higher than surface values (Table 4).

Shear-wave velocity: It is known that slag cement has a lower early strength and longer setting time (Wu et al. 1990). This is reflected by the approximately constant shear-wave velocity measured during the first two to three days (an early jump was measured during the first few hours, due to consolidation). A high rate of increase in velocity was observed afterwards, and lasted for approximately seven days as shown in Fig. 5(a).

ANALYSIS OF RESULTS

Results presented in the preceding sections point to multiple concurrent phenomena subjected to complex interactions. The following analysis assesses hypothesis of behavior that can account for observations made.

Sedimentation and Mixing Order

Results presented in Fig. 1 indicate that the delamination of bentonite particles (observed in test 1) is not readily reversed with the increased ionic concentration (test 2); however, initial lattice expansion is limited in high-concentration solutions (test 3). The final volume of the sediment reflects both particle hydration and the formation of different fabrics. For example, adding dry bentonite to a salt solution (test 3) may result in fact-to-face particle aggregation, whereas, gelation or the formation of a single floc that occupies the available volume may take place on prehydrated bentonite (test 2), leading to larger volume [edge-to-face and edge-to-edge arrangements; van Olphen (1977)]. Finally, a nearly dispersed structure with larger particle spacing is expected in the bentonite slurry without salt (test 1). The similarity between the sedimentation of attapulgite in water (test 1) and attapulgite in $CaCl_2$ solution (test 3) reflects the lack of substantial double-layer effects in attapulgite. The final volume of sediments is higher in the prehydrated attapulgite with salt added afterwards (test 2), probably due to gelation (scaffolding or haystack structure).

The results of clay-cement sedimentation tests resembled those of clay-salt tests. Cement hydration liberates ions almost immediately upon wetting (Fig. 4), affecting the hydration of bentonite. Therefore, dry-mixed bentonite and cement [Fig. 2(a)] is approximately the same as mixing bentonite with $CaCl_2$ solution [test 3, Fig. 1(a)]. Whereas, adding cement to prehydrated clay appears to be similar to adding salt [test 2, Fig. 1(a)]. However, the similarity between sedimentation results for prehydrated bentonite with salt (test 2) and wet-mixed

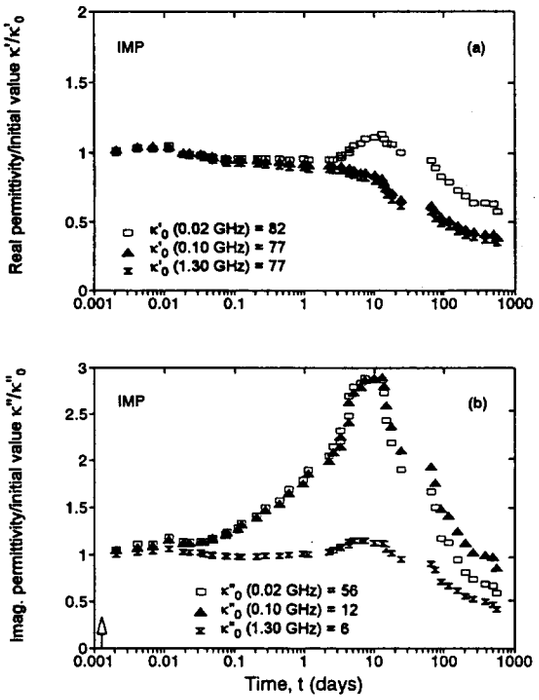

FIG. 8. Change in Complex Permittivity of Impermix with Hydration Time, at Three Frequencies: (a) Real; (b) Imaginary (Permittivity Values Are Normalized by Initial Values; Arrow Denotes Time of Temperature Peak)

bentonite-cement slurry does not imply equal fabric [pH is different; see microphotographs in Plee et al. (1990)]. The sedimentation rate is higher in dry-mixed slurries because of the large particle size of cement surrounded by dry or poorly hydrated clay particles. In wet-mixed slurries, the attraction of hydrated clay particles to cement produces large flocs, but with unit weight lower than cement; thus, there is a slower sedimentation rate. Due to the specific surface of bentonite compared to cement (at early stages of hydration), a small percentage of bentonite particles becomes attracted to cement. Yet, the presence of cement accelerates sedimentation, even though pH and κ'' changes start to manifest about 10 min later (Fig. 3). The presence of cement also shortens the sedimentation time in attapulgite-cement mixtures. However, in the wet-mixed slurry, partially unbundled attapulgite slows the rate of sedimentation.

Dielectric Permittivity

Suzuki et al. (1981) indicated that cement particles are covered with layers of calcium silicate hydrate at the beginning of cement hydration, which hide the increase in Ca^{++} ions. On the other hand, McCarter and Curran (1984) hypothesized that silica and lime form a coating around C_3S, which retards reaction. The results in this paper show that the presence of clays in soil-cement slurries further delays reactions and their manifestion, imposing a slower diffusion rate (compare Figs. 4, 6, and 7). In spite of the fact that water is immediately in contact with cement particles in wet-mixing, the availability of water is restricted, slowing hydration and delaying temperature rise (compare Figs. 4 and 6). In addition, hydrated clays act as semipermeable membranes (Fritz and Marine 1983; Mitchell 1993) and temporarily absorb the by-products of hydration, leading to a retardation in measured changes. The clay shield that forms during dry-mixing further delays the arrival of water to the cement, producing a longer dormant period [compare Fig. 3(a) for bentonite cement and Fig. 4 for cement alone]. Therefore, both dry-mixed and wet-mixed slurries delay hy-

dration and retard its manifestation. The lack of differences in pH and κ'' between the two mixing orders in attapulgite-cement slurries [Fig. 3(b)], suggests that cement particles have equal access to water in both cases. However, attapulgite also exhibits the retarding or buffering effect observed in bentonite.

Four stages can be distinguished in the plot of the imaginary permittivity versus time for cement and clay-cement slurries [Figs. 4(b), 6(b), and 7(b)]. During the first stage, the imaginary permittivity κ'' increases with time at a low rate confirming the "leaky" induction period that starts immediately after mixing. The second stage involves a much faster rate of increase in imaginary permittivity, suggesting the more direct exposure of cement to water and active hydration. We have observed that the higher the cement content, the higher the rate of increase in the imaginary permittivity during this stage. The values for κ'' remain high during the third stage. Finally, imaginary permittivity decreases due to the entrapment of ions and water into cementitous products. In these four stages, low-frequency results are similar to high-frequency κ'' but with higher values. The comparison of κ'' values in bentonite and attapulgite (Figs. 6 and 7) shows similar stages. It is concluded that the evolution of the imaginary permittivity in time is barely dependent on clay mineralogy and surface charge.

The overall decrease in high-frequency dielectric permittivity κ' with time for cement and clay-cement slurries points to two concurrent phenomena: the change of free water into bound water due to cement hydration, and a decrease in permittivity as a result of the increase in concentration (hydration water is less polarizable). At low frequencies (0.2 GHz), the real permittivity shows an early increase with time, reflecting the higher availability of mobile ions (e.g., liberated Ca^{++} in the dissolution of C_3S), the ability for increased spatial polarization [see also McCarter and Curran (1984)], and the increase in double-layer phenomena due to the increase in surface area (Plee et al. 1990). Similar differences between low 0.02 GHz and high 1.30 GHz frequencies are observed in water-salt solutions, e.g., KCl.

The complex permittivity response for impermix was different from that of bentonite cement and attapulgite cement. The longer hydration time of slag cement is responsible for the delay in reaction, which is implied by the position of the permittivity peak compared to cement and clay-cement slurries (compare Fig. 8 with Figs. 4, 6, and 7). It is important to recall that impermix is not a wet-mixed slurry; dry-mixing may also delay the rate of reaction as in bentonite [Fig. 3(a)] even though the manufacturer describes impermix as an attapulgite-base mixture.

Shear-Wave Velocity

The high early values of κ'' and the low rate of increase in the V_S of cement suggest that early stages of hydration do not contribute to the formation of a rigid, cemented network. However, the definite increase in V_S for cement paste after 0.1 day [Fig. 5(a)] occurs simultaneously with the final decay in permittivity. The match between the measurements of these physical properties, κ^* and V_S, confirms the fundamental dependency between chemical reactions (which affect polarizability and losses) and the development of rigidity (V_S) in cementitious materials.

In the case of soil-cement slurries, the increase in rigidity starts before the final decay in κ^* [Figs. 5(b), 6, and 7]. The increase in velocity V_S in clay-cement mixtures response to at least three simultaneous processes: the increase in effective stress due to the consolidation of the mixture under a 1.50 kPa load, the decrease in double-layer repulsion by the substitution of Na^+ for Ca^{++} in high concentration, and the increased rigidity of the mix as a result of cementation. Results for B-1-0.1-12 and B-1-1-23 show the prevailing effect of the last mechanism on shear-wave velocity.

Following the addition of cement to prehydrated bentonite, water in the double layer is liberated due to the cation exchange of Na^+ for Ca^{++}. A temporary decrease in the rigidity of the slurry is expected; however, no drop in shear-wave velocity was observed, probably due to the poor time resolution at very low values of velocity. Most likely, this stage occurs during mixing [see Jefferis (1982)].

The high final velocity of impermix reflect the high cement-clay ratio (up to 4:1). Once again, synchronous changes in electromagnetic and mechanical parameters confirm the interrelationship between the rate of chemical reactions and the change in mechanical properties of clay-cement slurries.

CONCLUSIONS

The availability of water for cement hydration is restricted in soil-cement slurries. In addition, hydrated clays act as semipermeable membranes that temporarily absorb hydration products leading to a retardation in measured changes. Therefore, the presence of clays in soil-cement slurries delays reactions and their manifestation, imposing slower diffusion rates.

Both imaginary permittivity and pH measurements reflect different reaction rates for different mixing orders in bentonite-cement slurries. In addition, sedimentation tests show that the mixing order alters the fabric of the mixture, both in attapulgite- and bentonite-based slurries.

The complex permittivity is a sensitive indicator of ongoing reactions. It reflects changes in the mobility of water, liberation and entrapment of ions, changes in specific surface, and variations in double-layer phenomena.

The increase in shear velocity in clay-cement mixtures responds to three simultaneous phenomena: the increase in effective stress due to consolidation, the decrease in double-layer repulsion by the substitution of Na^+ for Ca^{++} in high concentration, and the increased rigidity of the mix as a result of cementation. Early stages of hydration denoted by changes in complex permittivity do not contribute to the formation of a rigid, cemented network.

The simultaneous measurement of the electromagnetic complex permittivity and the shear-wave velocity provides complementary information on the fundamental dependency between chemical reactions, which affect polarizability and losses, physical changes, and the development of rigidity in cementitious materials.

ACKNOWLEDGMENTS

This study is part of a research program on wave-geomedia interaction and applications. Funding was provided by the Natural Sciences and Engineering Research Council of Canada (NSERC), Ottawa, Canada. Liquid Earth Support Inc., New York, and Floridin Co., Quincy, Florida, provided the raw materials.

APPENDIX I. REFERENCES

Berthaud, Y. (1991). "Damage measurements in concrete via an ultrasonic technique. I: Experiment." *Cement and Concrete Res.*, Vol. 21, 73–82.

Broderick, G. P., and Daniel, D. E. (1990). "Stabilizing compacted clays against chemical attack." *J. Geotech. Engrg.*, ASCE 116(10), 1549–1567.

Chapuis, P. R., Pare, J. J., and Loiselle, A. A. (1984). "Laboratory test on self hardening grouts for flexible cut-off walls." *Can. Geotech. J.*, Ottawa, Canada, Vol. 21, 185–191.

Chelkowski, A. (1980). *Dielectric physics*. Elsevier Scientific Publishing Co., New York, N.Y.

Fam, M., and Santamarina, J. C. (1995). "Study of geoprocesses with complementary mechanical and electromagnetic wave measurements in an oedometer." *Geotech. Testing J.*, 18(3), 307–314.

Fang, H. Y., Pamukcu, S., and Chaney, R. C. (1992). "Soil-pollution

effects on geotextile composite walls." *Slurry walls: design, construction, and quality control; ASTM STP 1129*, D. B. Paul, R. R. Davison, and N. J. Cavalli, eds., ASTM, Philadelphia, Pa.
Fritz, S. J., and Marine, I. W. (1983). "Experimental support for a predictive osmotic model of clay membranes." *Geochimica et Cosmochimica Acta*, Vol. 47, 1515–1522.
Hasted, J. B. (1973). *Aqueous dielectrics*. Chapman and Hall, London, England.
Jefferis, S. A. (1981). "Bentonite-cement slurries for hydraulic cut-offs." *Proc., 10th Int. Conf. on Soil Mech. and Found Engrg., Vol. 1*, 435–440.
Jefferis, S. A. (1982). "Effects of mixing on bentonite slurries and grouts." *Proc., Conf. on Grouting in Geotech. Engrg.*, W. H. Baker, ed., ASCE, New York, N.Y., 62–76.
Jefferies, S. A. (1992). "Contaminant grout interaction." *Geotech. Spec. Tech. Publ. No. 30; Grouting, soil improvement, and geosynthesis*, R. H. Borden, R. D. Holtz and I. Juran, eds., ASCE, New York, N.Y., 2(30), 1393–1402.
Kezdi, A. (1979). *Stabilized earth roads*. Elsevier Scientific Publication Co., Amsterdam, The Netherlands.
Laine, E. F., Dines, K. A., Okada, J. T., and Lytle, R. J. (1980). "Probing concrete with radio waves." *J. Geotech. Engrg.*, ASCE, 106(7), 759–766.
Lawrence, F. V., Young, J. F., and Berger, R. L. (1977). "Hydration and properties of calcium silicate pastes." *Cement and Concrete Res.*, Vol. 7, 369–378.
Leonards, G. A., Schmednecht, F., Chameau, J. L., and Diamond, S. (1985). "Thin slurry cutoff wall installed by the vibrated beam method." *Hydraulic barriers in soil and rock; ASTM STP-874*, A. I. Johnson, R. K. Frobel, N. J. Cavalli, and C. B. Petterson, eds., ASTM, Philadelphia, Pa., 34–44.
Matsufuji, Y., and Kawakami (1984). "A study on the evaluating method of setting condition of concrete mixtures by shear wave propagation characteristics." *Proc., 28th Japan Congr. on Mat. Res.*, Soc. of Mat. Sci., Kyoto, Japan, 121–126.
McCarter, W. J., and Curran, P. N. (1984). "The electrical response characteristics of setting cement paste." *Mag. of Concrete Res.*, 36(126), 42–49.
Mehta, P. K. (1986). *Concrete: structure, properties, and materials*. Prentice-Hall, Inc., Englewood Cliffs, N.J.
Millet, R. A., Perez, J. Y., and Davison, R. R. (1992). "USA practice slurry wall specifications 10 years later." *Slurry walls: design, construction, and quality control; ASTM STP 1129*, D. B. Paul, R. R. Davidson, and N. J. Cavalli, eds., ASTM, Philadelphia, Pa.
Mitchell, J. K. (1993). *Fundamentals of soil behavior*, 2nd Ed., John Wiley & Sons, Inc., New York, N.Y.
Mitchell, J. K., and Arulanandan, K. (1968). "Electrical dispersion in relation to soil structure." *J. Soil Mech. and Found. Div.*, ASCE, 94(2), 447–471.
Mitchell, J. K., and El Jack, S. A. (1965). "The fabric of soil-cement and its formation." *Proc., 14th Nat. Conf. on Clays and Clay Minerals*, Pergamon Press, Oxford, England, 297–305.
Moukwa, M., Brodwin, M., Christo, S., Chang, J., and Shah, S. P. (1991). "The influence of the hydration process upon microwave properties of cements." *Cement and Concrete Res.*, Vol. 21, 863–872.
Plee, D., Lebedenko, F., Letelier, M., and van Damme, H. (1990). "Microstructure, permeability and rheology of bentonite-cement slurries." *Cement and Concrete Res.*, Vol. 20, 45–61.
Roesler, S. K. (1979). "Anisotropic shear modulus due to stress anisotropy." *J. Geotech. Engrg.*, ASCE, 105(7), 871–880.
Sai, J. O., and Anderson, D. C. (1992). "Barrier wall materials for contaminant of dense non-aqueous phase liquid (DNAPL)." *Hazardous Waste and Hazardous Mat.*, 9(4), 317–330.
Santamarina, J. C., and Fam, M. (1995). "Changes in dielectric permittivity and shear wave velocity during concentration diffusion." *Can. Geotech. J.*, Ottawa, Canada, 32(4), 647–659.
Schultheiss, P. J. (1981). "Simultaneous measurements of P and S wave velocities during conventional laboratory soil testing procedures." *Marine Geotechnol.*, 4(4), 343–367.
Smith, S. S., and Arulanandan, K. (1981). "Relationship of electrical dispersion to soil properties." *J. Geotech. Engrg.*, ASCE, 107(5), 591–605.
Suzuki, K., Nichikawa, T., Hayashi, J., and Ito, S. (1981). "Approach by zeta potential on the surface change of hydration of C_3S." *Cement and Concrete Res.*, Vol. 11, 759–764.
Tamas, F. D. (1982). "Electrical conductivity of cement pastes." *Cement and Concrete Res.*, Vol. 12, 115–120.
Taylor, H. F. (1990). *Cement chemistry* Academic Press, London, England.
Trivedi, D. P., Holmes, R. G., and Brown, D. (1992). "Monitoring the in-situ performance of a cement/bentonite cut-off wall at low level waste disposal." *Cement and Concrete Res.*, Vol. 22, 339–349.
Van Olphen, H. (1977). *An introduction to clay colloid chemistry*, 2nd Ed., John Wiley & Sons, Inc., New York, N.Y.
Viggiani, G., and Atkinson, J. H. (1995). "Stiffness of fine-grained soils at very small strains." *Geotechnique*, London, England, 45(2), 249–265.
Wensink, W. A. (1993). "Dielectric properties of wet soils in the frequency range 1–3000 MHz." *Geophys. Prospecting*, Vol. 41, 671–696.
Wilding, C. R., and Double, D. D. (1984). "A study of inorganic and organic admixtures using combined calorimeter and ultrasonic pulse velocity technique." *The chemistry and chemistry-related properties of cement*, F. P. Glasser, ed., British Ceramic Society, Shelton, Stoke-on-Trent, England, 349–356.
Wu, X., Jiang, W., and Roy, D. M. (1990). "Early activation and properties of slag cement." *Cement and Concrete Res.*, Vol. 20, 961–974.
Xie, P., Gu, P., Xu, Z., and Beaudoin, J. J. (1993). "A rationalized A.C. impedence model for microstructural characterization of hydrating cement systems." *Cement and Concrete Res.*, Vol 23, 359–367.
Yong, R. N., and Phadungchewit, Y. (1993). "pH influence on selectivity and retention of heavy metals in some clay soils." *Can. Geotech. J.*, Ottawa, Canada, Vol., 30, 821–833.

APPENDIX II. NOTATION

The following symbols are used in this paper:

G = shear modulus;
G_S = specific gravity;
LL = liquid limit;
pH = −log (hydrogen ion concentration);
T = temperature;
t = time;
V_S = shear-wave velocity;
w/c = water-cement ratio;
κ' = real dielectric permittivity;
κ'' = imaginary dielectric permittivity;
κ^* = complex dielectric permittivity;
ρ = mass density; and
σ_v = vertical stress.